APEM journal
Advances in Production Engineering & Management
Volume 20 | Number 2 | June 2025 | pp 173–190
https://doi.org/10.14743/apem2025.2.534
ISSN 1854-6250
Journal home: apem-journal.org
Original scientific paper

Low-carbon multimodal vehicle logistics route optimization with timetable limit using Particle Swarm Optimization

Jiao, Z.H.[a], **Duan, H.W.**[a,*], **Zhou, Y.J.**[a], **Xiang, X.W.**[b]

[a]School of Management, Xihua University, Chengdu, Sichuan, P.R. China
[b]FAW Logistics (Chengdu) Co., Ltd, Chengdu, Sichuan, P.R. China

ABSTRACT

Optimizing the multimodal transport route for vehicles is crucial for reducing costs, enhancing efficiency, and minimizing emissions in the vehicle logistics industry. This study addresses several operational challenges, including seasonal fluctuations in vehicle sales, the scheduling of transportation modes, and client-specific order timing requirements. This paper presents a 0-1 integer programming model under carbon trading policy considering the timetable limit, with the objective of minimizing the aggregate costs of transportation, transshipment, short-term storage, time-window penalties, and carbon emissions. A linear weight reduction technique is employed to formulate the Improved Particle Swarm Optimization (IPSO) algorithm with dynamic inertia weights for model resolution. The model and algorithm's efficacy are validated by a real-world case study of multimodal transport in China. The results reveal that the IPSO algorithm reduced convergence times by 30.38 % and 17.78 % in off-season and peak season data, respectively, compared to the traditional PSO algorithm. Additionally, the optimized multimodal transport solution reduced unit costs by 19.3 % and 14.8 %, respectively. The findings indicate that transport timeliness significantly influences optimal route selection. Factors such as extended short-term storage duration, missed shipping schedules, and expedited orders compel multimodal transport to shift toward road transport. An increase in carbon trading prices effectively encourages a shift from road transport to multimodal transport; however, excessively high carbon trading prices fail to regulate this transition. Furthermore, as transport distance increases, the transport costs and carbon emission advantages associated with multimodal transport also increase correspondingly. This research advances multimodal logistics by integrating seasonal variations and carbon trading into a novel optimization framework.

ARTICLE INFO

Keywords:
Low-carbon multimodal transport;
Vehicle logistics;
Route optimization;
Timetable limit;
Particle swarm optimization

**Corresponding author:*
vividyhua@mail.xhu.edu.cn
(Duan, H.W.)

Article history:
Received 19 November 2024
Revised 27 June 2025
Accepted 30 June 2025

1. Introduction

As per the figures published by the China Association of Automobile Manufacturers (CAAM) on January 11, 2024, China's automobile production and sales totaled 30.161 million and 30.094 million units in 2023, maintaining the world's leading position for several straight years. All vehicles manufactured and sold in China during the year were conveyed via vehicle logistics. Vehicle logistics is a logistics that takes the vehicle as the goods, responds quickly and delivers on time according to the requirements of the delivery date and delivery place of the customer order. Nevertheless, regulatory modifications in several policies have led to a substantial decline in the amount of road transport for vehicles.

In 2020, the Chinese government suggested a dual-carbon policy to foster high-quality and sustainable development [1, 2]. In 2011, the Chinese government implemented a carbon trading system, and in 2021, the national carbon emissions trading market was officially inaugurated to incentivize firms to diminish carbon emissions [3]. The transport sector contributes 16.5 % of worldwide carbon dioxide greenhouse gas emissions, primarily from road transport. Consequently, conventional road transport methods are unable to satisfy varied customer expectations, and vehicle logistics confronts the significant task of evolving towards a high-quality development phase.

Multimodal transport integrates many transport modes, enhancing efficiency, lowering costs, and reducing carbon emissions [4-6]. China's multimodal vehicle transport has advanced swiftly over the past decade; however, numerous challenges persist, including congestion in the buffer zone during peak vehicle sales seasons, stringent limitations on the departure schedules of rail and maritime transport, and the nascent integration of the transport sector into the carbon trading framework.

Multimodal transport elements mutually constrain one another and significantly influence the objectives of vehicle logistics businesses and clients regarding transit costs, duration, and carbon emissions. Nevertheless, the existing studies seldom consider the above factors comprehensively in the modeling process. Moreover, prior research has inadequately addressed the off-peak periods of vehicle sales and the limitations of transport mode schedules and has not been effectively aligned with carbon pricing plans. Consequently, it is highly significant to scientifically address the challenges of low-carbon multimodal transport of vehicles under scheduling restrictions and to offer effective transport solutions for the advancement of the vehicle logistics sector.

This paper contributes to the state-of-the-art research in three ways: First, we assess the influence of vehicle sales off-season and peak season on the cached links at the nodes and subsequently examine the difference of the schedule period and the schedule of each line, considering the specialized nature of vehicle transport. The conclusion shows that both short-term storage and awaiting a shift connection diminish the overall cost benefits of multimodal transport to differing extents. Secondly, we examine the carbon emissions associated with each segment of vehicle multimodal transport and, in conjunction with China's carbon trading policy, demonstrate that a moderate increase in carbon trading prices will effectively foster the advancement of low-carbon multimodal transport, while an excessively elevated carbon trading price will fail to function as a regulatory mechanism. Thirdly, we comprehensively evaluate all elements in the development of the vehicle multimodal transport model, examining real cases involving multiple dealers. We conclude that variations in transport distance among dealers also influence the selection of transport options. As transport distance increases, the benefits in terms of transport cost and carbon emission cost derived from multimodal transport also increase, whereas the advantage concerning time window penalty cost diminishes.

The remainder of the document is structured as follows. Section 2 presents a concise literature review. Section 3 constructs a model for comprehensive vehicle multimodal optimization. Section 4 designs an Improved Particle Swarm Optimization (IPSO) algorithm with dynamic inertia weights. Section 5 conducts a case study to validate the model and methodology, along with a sensitivity analysis. Section 6 concludes the findings.

2. Literature review

Researchers have performed comprehensive studies on the optimization of multimodal transport routes [7, 8]. The optimal objectives of the developed model in this work can be primarily categorized into two types: one is multi-objective optimization with the objective of minimizing transport cost and transport time. On that basis, several researchers additionally regard the expenses associated with container utilization and carbon emissions as optimization objectives. The alternative is a single-objective optimization that accounts for many cost categories and seeks to minimize the overall cost, primarily focusing on transportation costs, time costs, and carbon emission costs [9-11]. Liu *et al.* examine the constraints of departure timing in railway and river transportation concerning time expenditure [12]. In optimizing multimodal

routes for vehicle transport, most contemporary academics develop integer programming models with the minimization of total cost as the optimization target [13-15]. Nevertheless, only a limited number of scholars have examined the short-term storage of products at intermediate nodes and have not conducted further analysis on the phenomenon of cargo caching [16].

The punctuality of cargo transport is a critical determinant of logistics service quality, influenced by order shipment timing, delivery time frame requirements, and the transport mode schedule. The time window is an efficient strategy in transportation planning to ensure timely deliveries and minimize transportation expenses. Certain studies have established rigid time window limits; nevertheless, in practical transportation scenarios, such constraints may render the problem challenging or insurmountable. Within a flexible time frame, commodities may be supplied over an extensive period, and late deliveries incur associated expenses [17, 18]. In comparison to temporal frameworks, a limited number of researchers have examined transportation transitions.

The subject of carbon emissions has garnered the attention of numerous researchers due to global warming. Multimodal transport is not only more cost-effective than road freight transport but also more environmentally sustainable [19]. Wang *et al.* introduced a standardized methodology for calculating multimodal transport congestion, carbon emissions, and related issues [20, 21]. Yin *et al.* investigated the synergistic impacts of railway freight subsidies and carbon trading mechanisms within low-carbon transport networks [22].

The existing multimodal transport literature has produced significant research outcomes in modeling and optimization methods. Nonetheless, the subsequent topics remain unaddressed in the current literature: This study examines multimodal transport from the viewpoint of vehicle shippers, focusing on the effects of seasonal fluctuations in vehicle sales on short-term storage logistics. Secondly, in view of the problems such as schedule limit, carbon pricing policy, order time requirement, the transport route is optimized through reasonable modeling. This paper focusses on the optimization of vehicle multimodal transport paths while considering timetable constraints within a low-carbon context, thereby contributing to the existing research in vehicle logistics and multimodal transport path optimization.

3. Description and modeling

3.1 Description of the problem

In this study, a multimodal transport operator carries a batch of vehicles as cargo from the starting point O to a number of various end points D through the multimodal transport network $G = \{N, L, M\}$, where N denotes the set of nodes of the multimodal transport network, $i, j, k \in N = \{1,2, \dots, n\}$, $i \neq j \neq k$; L denotes the set of transport arcs between two nodes, $L = \{ l_{i,j} \mid \forall i, j \in N \}$; M denotes the set of modes of transport, $m, n, h \in M, m, n = 1$ or 2 or 3, $h = 2$ or 3 (1 stands for road transport, 2 stands for rail transport, and 3 stands for waterway transport), $m \neq n$ and $h \neq n$.

Merchandise may be transshipped at a node, and between two nodes, many transport routes are available, differing in distance, duration, cost, economies of scale discount factors, and carbon emissions. Each dealer possesses a designated shipment time and a comprehensive transit time requirement for the items. Following transshipment at the transit node, they must await the subsequent shift to the next node and will face a window penalty cost if they arrive outside the permissible time window. Vehicle sales have relatively obvious off and peak seasons, limited by the processing capacity of the platform/port cache area, sales peak season cache area congestion will produce a longer short-term storage time. Consequently, it is essential to analyze the differing dealer demands and short-term storage times during the off and peak sales seasons in a detailed manner. Under the carbon trading policy, the multimodal transport operator possesses a specified quantity of carbon emission allowances. If the operator's carbon emissions exceed this allowance, it must purchase additional credits at the carbon trading unit price to compensate for the surplus emissions incurred during multimodal transport. Conversely, if emissions are below the allowance, the operator may sell the surplus carbon emission credits. The objective function, comprising

transport cost, transshipment cost, short-term storage cost, time-window penalty cost, and carbon emission cost, is utilized to determine the transport scheme that minimizes the total expenditure for suppliers in delivering the vehicle to each dealer. Fig. 1 illustrates the multimodal shipping network for vehicles.

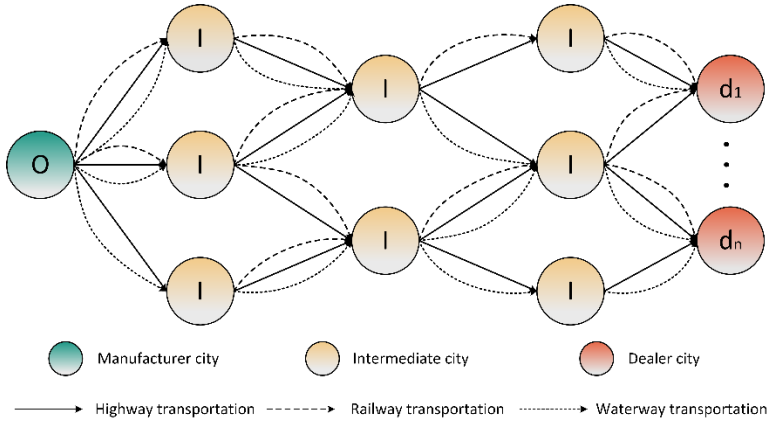

Fig. 1 Multimodal transport process for vehicle logistics

This paper presents the basic assumptions to facilitate modeling and enhance the operability of the model.

- The nodes' locations and capacities are established, along with the distances and reachability among all nodes,
- The total production of the vehicle and the dealers' demand are specified,
- Shipments are indivisible, and each dealer's shipment cannot be divided during transport,
- Only one mode of transport is permitted between two adjacent nodes,
- Mode transitions occur solely at nodes and can happen at most once at any given node,
- After transshipment at the transit node, the nearest shift is utilized to proceed to the subsequent node,
- Waiting during transit is prohibited, except when necessitated by shift restrictions.

3.2 Model symbols and parameters

The symbols in the vehicles multimodal route optimization model with timetable constraints in a low carbon context are described in Table 1.

Table 1 Description of sets, parameters and decision variables

Set	
N	A collection of nodes in a multimodal transport network
L	A collection of arcs of a multimodal transport network
M	A collection of transport modes
D	A collection of dealers, d denotes dealers that $d \in D,\ D \in N$
U	A collection of schedules, u denotes the schedule, $u \in U$
Parameters	
a^m	Discount factor for economies of scale in transport costs arising from the use of m transport modes between transport nodes
Q	Manufacturer's output(car)
Q_{ij}^m	Flow (car) between node i and node j choosing transport mode m
Q_d	Dealer d's vehicle demand (car)
l_{ij}^m	Nodal city i transport distance (km) to nodal city j by selecting transport mode m
t_{od}	The moment of shipment of the goods requested by the distributor d
t_{id}	Total time (h) taken for goods from distributor d to reach node i
B_{ijd}^{mn}	Distributor d Nearest moment of departure of transport mode n after conversion of transport mode m to transport mode n at node i for goods in transit from node i to node j
B_{ijd}^{mnu}	Distributor d The first departure moment of the mode of transport n at u after the conversion of the mode of transport m into the mode of transport n at the node i for the shipment transiting from the node i to the node j

T_{ijd}^{mn}	Distributor d The moment after the conversion of the shipment from transport mode m to transport mode n at node i for shipments transiting from node i to node j
t_{ij}^{m}	Node i Selection of mode of transport m Transport time (h/km) per unit distance to node j
t_i^{mn}	Conversion time (h) for node i to convert transport method from m to n
t_i^S	Short-term storage time (h) at node i
t_i^{Sf}	Duration of free storage period (h) at node i
T_d^{max}	Upper limit of the soft time window (h) for goods from distributor d
T_d	Total time (h) taken for goods from distributor d to reach destination
c_{ij}^{m}	Node i Unit transport cost (CNY/car·km) for transport mode m to node j
c_i^{mn}	Unit conversion cost (CNY/car) at node i to convert mode of transport from m to n
c_i^S	Unit short-term storage costs (CNY/car·h) at node i
c_t^p	Penalty cost (CNY/car·h) per unit of time for delayed arrival of the vehicle at the end of the journey
W	Carbon market unit price (CNY/kg)
e_m	Mode of transport m Carbon emissions (kg/car·km) per unit of transport during transport
e_i^{mn}	Carbon emissions (kg/car) per unit of transport changed from m to n at node i
E_{max}	Multimodal transport operator CO2 emission allowances (kg)
E_d	Carbon dioxide emissions (kg) from full transport of goods by distributor d
P_{ij}^{m}	Maximum transport volume (car) from node i to node j using transport mode m
V_i	Capacity (car) of node i
Decision variables	
x_{ijd}^{m}	The node i carries the goods of the dealer d to the node j using the mode of transport m taking the value of 1 and 0 otherwise, $i \neq j$
y_{id}^{mn}	The node i converts the goods of the distributor d using the mode of transport m to the mode of transport n taking the value 1, otherwise 0, $m \neq n$

3.3 Process and cost analysis

The Vehicle Logistics link is set up with a dedicated railway/waterway cache area, which is more efficient, however, limited by the processing capacity of the cache area, the off and peak season of the vehicle sales has a significant impact on the outbound time of the cache area. Therefore, to ensure the rationality of the process as well as to avoid double-counting, this paper retains the articulation time of waiting shifts at the nodes and generates a short-term storage link only in the cache before outbound transshipment. As shown in Fig. 2, the multimodal transport process for Vehicle Logistics includes inter-node transport, short-term storage at nodes, transshipment at nodes, and waiting for the nearest shift, which generates the following five types of costs: transport costs, short-term storage costs, transshipment costs, time-window penalty costs, and carbon emission costs.

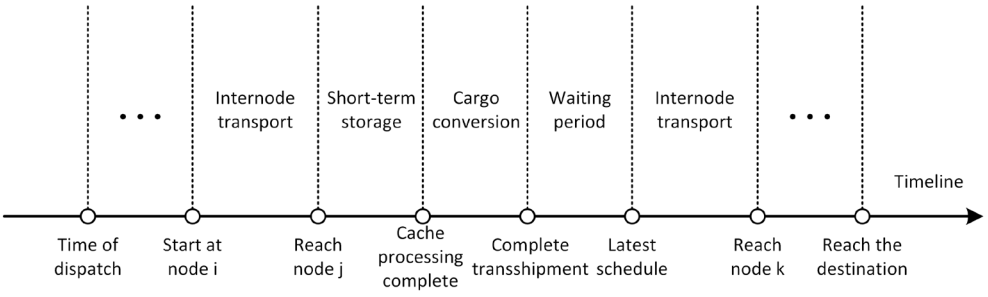

Fig. 2 Multimodal transport process for vehicle logistics

(1) Transport costs C_1. The transport costs for each route segment can be calculated from data on cargo demand, unit shipping price, transport distances, and discount coefficients for transport costs for economies of scale, with the formulas specified below:

$$C_1 = \sum_{d \in D} \sum_{\mathrm{m} \in M} \sum_{i,j \in N} Q_d \cdot c_{ij}^{\mathrm{m}} \cdot l_{ij}^{\mathrm{m}} \cdot a^{\mathrm{m}} \cdot x_{ijd}^{\mathrm{m}} \tag{1}$$

(2) Transshipment cost C_2. The transhipment cost at each node can be calculated by the cargo demand, unit transhipment price, the formula is specified as follows:

$$C_2 = \sum_{d\in D}\sum_{m,n\in M}\sum_{i\in N} Q_d \cdot c_i^{mn} \cdot y_{id}^{mn} \tag{2}$$

(3) Short-term storage cost C_3. The short-term storage cost at each node is mainly affected by the demand for goods, unit short-term storage cost, short-term storage time, and free storage period, and the formula is specified as follows:

$$C_3 = \sum_{d\in D}\sum_{h,n\in M}\sum_{i\in N} Q_d \cdot c_i^S \cdot max\left(t_i^S - t_i^{Sf}, 0\right) \cdot y_{id}^{hn} \tag{3}$$

(4) Time window penalty cost C_4. The time window penalty cost is determined by the demand for goods, the unit time penalty cost, the total time spent on transport, and the dealer time window, which is expressed as follows:

$$C_4 = \sum_{d\in D} Q_d \cdot c_t^p \cdot max(T_d - T_d^{max}, 0) \tag{4}$$

$$\begin{aligned} T_d = &\sum_{m\in M}\sum_{i,j\in N} t_{ij}^m \cdot l_{ij}^m \cdot x_{ijd}^m + \sum_{n,h\in K}\sum_{j\in N} t_j^S \cdot y_{jd}^{hn} \\ &+ \sum_{m,n\in M}\sum_{j\in N} t_j^{mn} \cdot y_{jd}^{mn} + \sum_{m,n,h\in M}\sum_{i,j,k\in N} \left(B_{jkd}^{mn} - T_{jkd}^{mn}\right) y_{jd}^{mn} \end{aligned} \tag{5}$$

The formula for T_d consists of the following four parts: transport time, short-term storage time, transit time, and waiting time due to schedule constraints. Because of the long rail/waterway schedule intervals and the fact that most of the lines are operating on a fixed number of days per week, the schedule is based on a one-week (168 h) cycle. Where B_{jkd}^{mn} is calculated from Eqs. 6 and 7.

$$T_{jkd}^{mn} = \begin{cases} t_{od} + t_{id} + t_{ij}^m \cdot l_{ij}^m + t_j^S \cdot y_{jd}^{hn} + t_j^{mn}; \\ t_{od} + t_{id} + t_{ij}^m \cdot l_{ij}^m + t_j^S \cdot y_{jd}^{hn} + t_j^{mn} \le 168, i,j \in N, m,n,h \in M \\ mod\left(\left(t_{od} + t_{id} + t_{ij}^m \cdot l_{ij}^m + t_j^S \cdot y_{jd}^{hn} + t_j^{mn}\right), 168\right); \\ t_{od} + t_{id} + t_{ij}^m \cdot l_{ij}^m + t_j^S \cdot y_{jd}^{hn} + t_j^{mn} \ge 168, i,j \in N, m,n,h \in M \end{cases} \tag{6}$$

$$B_{jkd}^{mn} = \begin{cases} B_{jkd}^{mn1}; T_{jkd}^{mn} \le B_{jkd}^{mn1} or T_{jkd}^{mn} \ge B_{jkd}^{mnU} \\ B_{jkd}^{mn2}; B_{jkd}^{mn1} \le T_{jkd}^{mn} \le B_{jkd}^{mn2} \\ \vdots \\ B_{jkd}^{mnu}; B_{jkd}^{m,n,u-1} \le T_{jkd}^{mn} \le B_{jkd}^{mnu} \\ \vdots \\ B_{jkd}^{mnU}; B_{jkd}^{m,n,U-1} \le T_{jkd}^{mn} \le B_{jkd}^{mnU} \end{cases} \tag{7}$$

(5) Cost of carbon emissions C_5. This paper calculates the cost of carbon emissions based on the carbon trading system, which can be calculated by carbon dioxide emissions, carbon trading market unit price, carbon dioxide emission quotas, the formula is specified as follows:

$$C_5 = \sum_{d\in D} W \cdot E_d - WE_{max} \tag{8}$$

$$E_d = \sum_{m,n\in M}\sum_{i,j\in N} \left(Q_d \cdot l_{ij}^m \cdot e_{\mathrm{m}} \cdot x_{ijd}^m + Q_d \cdot e_i^{mn} \cdot y_{id}^{mn}\right) \tag{9}$$

3.4 Modeling

The symbols in the vehicles multimodal transport path optimization model with timetable constraints in a low carbon context are described in Table 1.

$$MinC_{total} = C_1 + C_2 + C_3 + C_4 + C_5 \tag{10}$$

$$0 \le a^m \le 1 \tag{11}$$

$$Q \geq \sum_{d \in D} Q_d \tag{12}$$

$$Q_{ij}^m = \sum_{d \in D} Q_d x_{ijd}^m \leq P_{ij}^m, \forall i, j \in N, m \in M \tag{13}$$

$$Q_{ij} = \sum_{d \in D} \sum_{m \in M} Q_d x_{ijd}^m \leq V_i, \forall i, j \in N \tag{14}$$

$$B_{jkd}^{mn} - T_{jkd}^{mn} \geq 0, \forall i、\ j、\ k \in N; \forall m, n \in M; \forall d \in N \tag{15}$$

$$x_{ijd}^m, y_{id}^{mn} \in \{0,1\} \tag{16}$$

$$\sum_{m \in M} x_{ijd}^m = 1, when\ i, j\ were\ defined \tag{17}$$

$$\sum_{m,n \in M} y_{id}^{mn} = 1, when\ i\ was\ defined \tag{18}$$

$$x_{ijd}^m + x_{jkd}^n \geq 2y_{jd}^{mn}, \forall i, j, k \in N; \forall m, n \in M; \forall d \in N \tag{19}$$

Eq. 10 denotes the minimum total cost of multimodal transport of the vehicle, which is the objective function of the model, and it mainly includes transport, transshipment, short-term storage, time window penalty and carbon emission cost. Eq. 11 denotes the range of values of the discount factor of the economy of scale transport cost. Eq. 12 denotes that the output of the manufacturer is not less than the sum of the demand of all dealers. Eq. 13 denotes that the traffic passing through the nodes between node i to node j indicates that the flow between node i and node j does not exceed the maximum transport volume of the mode of transport between the nodes. Eq. 14 indicates that the total flow through any transport node does not exceed the capacity of the transport node. Eq. 15 ensures that the cargo transit operation can be completed before the departure of the shift. Eq. 16 indicates the value of the decision-making variables. Eq. 17 indicates that the mode of transport cannot be changed halfway in the process of transport from node i to node j. Eq. 18 indicates that node i can switch the mode of transport, but only once. Eq. 19 denotes the uninterrupted transport equation for the vehicle.

4. Design of solving algorithm

4.1 Particle swarm optimization algorithm

The multimodal transport route optimization model established in this paper involves multiple intermediate variables, classifying it as a typical NP-Hard problem. Heuristic algorithms have excellent performance in combinatorial optimization and are widely applied to such optimization problems. Particle Swarm Optimization (PSO), an intelligent population-based stochastic optimization algorithm, is recognized as one of the most effective methods for addressing optimization problems developed in recent decades [23]. The particle swarm algorithm models flocking behavior by representing particles as massless entities, each assigned initial positions and velocities within the solution space. It iteratively utilizes a fitness function to identify an optimal solution.

The particle code is denoted by a_i^n, e.g., $a_i^2 = 3$ indicates that the transport path of the second dealer is the third in the sequence of all the reachable paths from the manufacturer to the dealer. The transport modes are denoted by 1, 2 and 3, which correspond to road transport, railway transport and waterway transport, respectively, as shown in Fig. 3. For the global optimal solution and the corresponding particle i in the particle swarm after t iterations, the optimal path corresponding to each dealer in the particle swarm is back-projected through particle i, and the transport nodes of the optimal path as well as the transport modes are combined to obtain the transport scheme of each dealer.

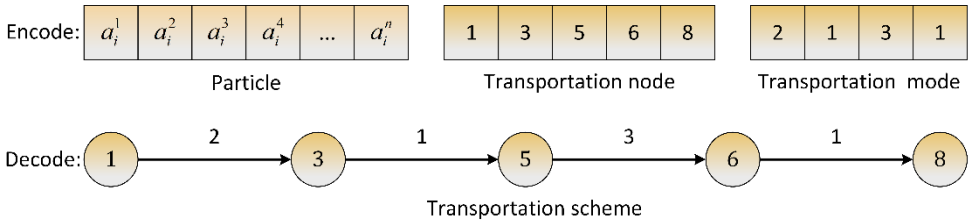

Fig. 3 Encoding and decoding

4.2 Dynamic inertia weights design

PSO exhibits rapid convergence and requires fewer parameters; however, it is prone to issues such as a tendency to converge to local optima, a reduction in convergence speed during later stages, and the risk of premature convergence. The inertia weight size reflects the extent to which the particle's current speed is retained. It is evident that the particle speed significantly influences the algorithm's global convergence, as demonstrated by Eq. 23. However, the inadequate control of particle speed results in the basic particle swarm algorithm lacking robust local search capabilities.

To enhance the balance between global and local search performance in PSO and to minimize the number of iterations, researchers have incorporated linearly decreasing inertia weights into the algorithm model. This modification enables particles to exhibit varying exploration capabilities throughout the evolutionary process [24]. Therefore, this paper adopts the linear decreasing weight strategy (LDW) to update the inertia weight factor w, so that it can be dynamically adjusted with the search process: at the beginning of the algorithm, a larger positive value can be given to w, so that each particle can quickly detect a better region within the global range, and as the search proceeds, w can be made to decrease gradually in a linear fashion, so that the algorithm can have a larger probability of converging to the position of the globally optimal solution. The expression is as follows:

$$w = w_{max} - \frac{(w_{max} - w_{min}) \cdot t}{T_{max}} \tag{20}$$

T_{max} denotes the maximum number of iterations, w_{min} denotes the minimum inertia weight, w_{man} denotes the maximum inertia weight, t denotes the current number of iterations.

4.3 Dynamic inertia weighted particle swarm optimization algorithm flow

Based on the above description, the IPSO flow designed in this study is shown in Fig. 4, where the algorithm solves under each inertia weight until it reaches the maximum number of iterations, and finally outputs the optimal solution.

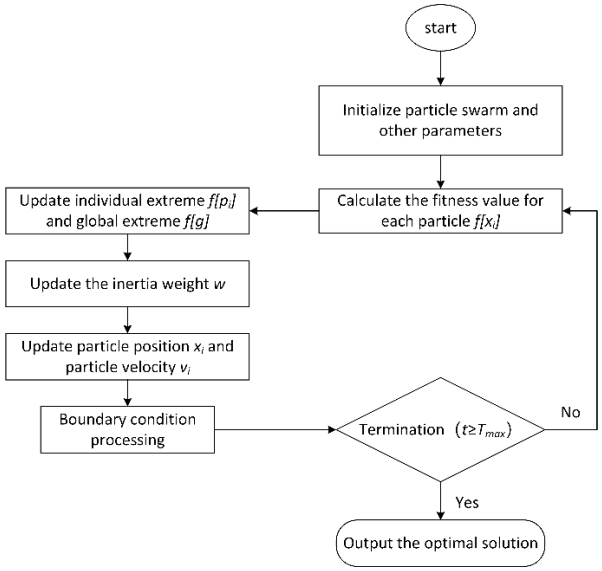

Fig. 4 IPSO flow chart

The specific steps of the algorithm are as follows. Step 1: Initialize the particle swarm as well as the parameters. Step 2: Record the fitness value of each particle $f[x_i]$ by optimization under constraints using c_{total} in Eq. 10 as a cost function for IPSO. Step 3: For each particle, update $f[p_i]$ and $f[g]$ with its fitness value by comparing it with the individual extreme value $f[p_i]$ and global extreme value $f[g]$. Step 4: Update the inertia weights w by Eq. 20. Step 5: Update the position x_i and velocity v_i of the particles. Step 6: Perform boundary condition processing to judge whether x_i and v_i are out of the specified range. Step 7: Judge whether the termination condition of the algorithm is satisfied, if not, return to step 2; if yes, end the algorithm and output the optimal solution.

5. Empirical case studies

5.1 Case descriptions

FAW Logistics Co. is a company mainly engaged in comprehensive vehicle logistics services, has established many logistics bases in China and formed a logistics network covering the whole country. The carrier needs to transport a batch of goods from Changchun to each dealer, and the short-distance transport from the distribution center to each dealer uses road transport. As shown in Fig. 5, Considering the geographical and economic distribution, this paper focuses on multimodal transport networks in the East China region of the Chinese mainland, selecting the top four prefecture-level city distributors with the highest demand in each province for analysis. Changchun, the node where the main plant is located, is chosen as the departure point, numbered O. The nodes where the seven distribution centers are located are numbered N_1 to N_7 ; the 21 dealers involved are divided into two categories, the first category of dealers is located in the distribution center node, with a total of 6 dealers, numbered $N_2(d_1)$ to $N_7(d_6)$; the second category of dealers is located in the nodes other than the manufacturer and the distribution centers, with a total of 15 dealers, numbered d_7 to d_{21}. Referring to the vehicle sales data on the official website of CAAM, the ratio of dealers' demand in peak seasons is set as 0.296 as the average value in the past three years.

The actual distances of different modes of transport between nodes were obtained according to Gaode Map, China Railway Information Network and Waterway Network, as shown in Table 2.

Based on the enterprise's actual data and the number of associated facilities and equipment, determine the maximum annual flow of various transport modes between the nodes, as illustrated in Table 3. The annual output of Node O is 1.1 million vehicles, representing the maximum annual capacity for the vehicle at each node, as detailed in Table 4.

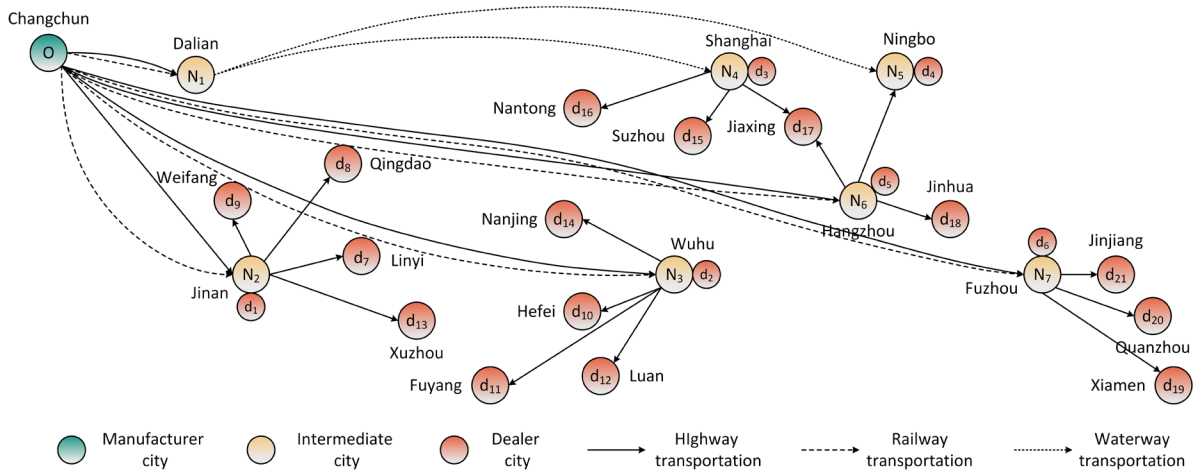

Fig. 5 Multimodal transport network for vehicles in East China

Table 2 Distance data for different modes of transport between nodes

Node-to-Node	Transport distance (km)			Node-to-Node	Transport distance (km)		
	Highway	Railway	Waterway		Highway	Railway	Waterway
O→N_1	679	700	-	N_3→d_{12}	234	-	-
O→N_2	1245	1346	-	N_3→d_{14}	101	-	-
O→N_3	1894	2138	-	N_4→$N_4(d_3)$	0	-	-
O→N_6	2031	2466	-	N_4→d_{15}	100	-	-
O→N_7	2687	3040	-	N_4→d_{16}	127	-	-
N_1→N_4	-	-	1022	N_4→d_{17}	98	-	-
N_1→N_5	-	-	1087	N_5→$N_5(d_4)$	0	-	-
N_2→$N_2(d_1)$	0	-	-	N_6→$N_6(d_5)$	0	-	-
N_2→d_7	236	-	-	N_6→N_5	156	-	-
N_2→d_8	352	-	-	N_6→d_{17}	84	-	-
N_2→d_9	208	-	-	N_6→d_{18}	166	-	-
N_2→d_{13}	320	-	-	N_7→$N_7(d_6)$	0	-	-
N_3→$N_3(d_2)$	0	-	-	N_7→d_{19}	254	-	-
N_3→d_{10}	150	-	-	N_7→d_{20}	178	-	-
N_3→d_{11}	352	-	-	N_7→d_{21}	187	-	-

Table 3 Flow constraint for different modes of transport between nodes

Node-to-Node	Flow Constraint (car)			Node-to-Node	Flow Constraint (car)		
	Highway	Railway	Waterway		Highway	Railway	Waterway
O→N_1	75,000	75,000	-	N_3→d_{12}	4000	-	-
O→N_2	75,000	75,000	-	N_3→d_{14}	14,000	-	-
O→N_3	65,000	65,000	-	N_4→$N_4(d_3)$	35,000	-	-
O→N_6	35,000	35,000	-	N_4→d_{15}	12000	-	-
O→N_7	20000	20000	-	N_4→d_{16}	7000	-	-
N_1→N_4	-	-	60,000	N_4→d_{17}	7000	-	-
N_1→N_5	-	-	20000	N_5→$N_5(d_4)$	25,000	-	-
N_2→$N_2(d_1)$	25,000	-	-	N_6→$N_6(d_5)$	25,000	-	-
N_2→d_7	10000	-	-	N_6→N_5	25,000	-	-
N_2→d_8	10000	-	-	N_6→d_{17}	7000	-	-
N_2→d_9	7000	-	-	N_6→d_{18}	7000	-	-
N_2→d_{13}	20000	-	-	N_7→$N_7(d_6)$	7000	-	-
N_3→$N_3(d_2)$	35,000	-	-	N_7→d_{19}	10000	-	-
N_3→d_{10}	13,000	-	-	N_7→d_{20}	4000	-	-
N_3→d_{11}	4000	-	-	N_7→d_{21}	4000	-	-

Table 4 Capacity constraint at each node

Node	Capacity Constraint (car)	Node	Capacity Constraint (car)	Node	Capacity Constraint (car)
O	1,000,000.	$N_4(d_3)$	302688	d_{13}	20000
N_1	700000	$N_5(d_4)$	384196	d_{14}	15000
N_2	394164	$N_6(d_5)$	107244	d_{15}	15000
N_3	74124	$N_7(d_6)$	178452	d_{16}	10000
N_4	302688	d_7	10000	d_{17}	10000
N_5	384196	d_8	10000	d_{18}	10000
N_6	107244	d_9	10000	d_{19}	10000
N_7	178452	d_{10}	15000	d_{20}	10000
$N_2(d_1)$	394164	d_{11}	10000	d_{21}	10000
$N_3(d_2)$	74124	d_{12}	10000		

The first three quarters of vehicle sales are off-season, and the fourth quarter is peak season. The demand of each dealer in the off-peak sales season is shown in Table 5. The average demand ratio of dealers during peak seasons in the past three years is set at 0.296. Therefore, in the specific case study, Tables 3 and 4 are correspondingly split according to this sales ratio. The data comes from the actual operation of the enterprise and the official website of CAAM.

Table 5 Dealer sales off and peak demand

Node	Quantity demanded (car)		Node	Quantity demanded (car)	
	Off-season	Peak season		Off-season	Peak season
$N_2(d_1)$	15779	6633	d_{12}	1323	556
$N_3(d_2)$	7891	3318	d_{13}	12346	5191
$N_4(d_3)$	23896	10047	d_{14}	7179	3018
$N_5(d_4)$	19170	5831	d_{15}	6708	2819
$N_6(d_5)$	15841	6661	d_{16}	3675	1545
$N_7(d_6)$	3466	1457	d_{17}	2546	1071
d_7	5326	2239	d_{18}	2905	1222
d_8	4456	1873	d_{19}	4064	1709
d_9	3663	1540	d_{20}	1531	644
d_{10}	7062	2962	d_{21}	653	275
d_{11}	1533	645			

The unit transport costs, transport time per unit distance, carbon emissions per unit of transport, and the discount factor for economy of scale transport costs for different modes of transport are shown in Table 6. The data were obtained from the current transport costs of enterprises, the China Transport Yearbook, the IPCC Guidelines for National Greenhouse Gas Inventories, and studies in the literature at [25].

Table 6 Summary of data relating to transport by different modes of transport

Mode of Transportation	Highway	Railway	Waterway
Unit freight (¥/car·km)	2.0 (distance ≤ 500km) 1.8 (distance > 500km)	1.6 (distance ≤ 500km) 1.4 (distance > 500km)	1.2 (distance ≤ 500km) 1.0 (distance > 500km)
Unit transit time (h/km)	1/90	1/70	1/34
Carbon emissions (kg/car·km)	0.364	0.035	0.101
Cost discount factor	0.8	0.6	0.4

The unit transfer cost, transfer time and unit transfer carbon emission of transfer between different modes of transport are shown in Table 7. The data were obtained from the actual operation data of enterprises and the research in literature [24, 25].

Table 7 Summary of data related to transhipment by different modes of transport

Mode of Transshipment	Highway-Railway	Highway-Waterway	Railway-Waterway
Unit freight (¥/car)	80	180	240
Transit time (h)	9	12	24
Carbon emissions (kg/car)	2.27	3.31	2.86

The railway/waterway schedules for vehicle logistics are shown in Table 8. Road transport departure time is implemented according to the whole point. The data comes from China Railway Special Cargo Logistics Co., Ltd (CRSCL), the actual operation data of the enterprise. In order to facilitate the model calculation, set the moment of shipment required by each distributor as 156:00 (12:00 on Friday).

The timeliness requirements for each distributor are shown in Table 9, with data derived from the company's current timeliness standards.

Table 8 Railway and waterway schedules between nodes

Node-to-Node	Railway	Waterway
$O \rightarrow N_1$	12:00, 36:00, 60:00, 84:00, 108:00, 132:00	-
$O \rightarrow N_2$	36:00, 108:00	-
$O \rightarrow N_3$	60:00, 132:00	-
$O \rightarrow N_6$	36:00, 84:00, 132:00	-
$O \rightarrow N_7$	36:00, 108:00	-
$N_1 \rightarrow N_4$	-	36:00, 108:00, 156:00
$N_1 \rightarrow N_5$	-	36:00, 108:00, 156:00

Table 9 Distributor time windows by distributor

Node	Upper Limit of Soft Time Window (h)	Node	Upper Limit of Soft Time Window (h)
$N_2(d_1)$	115.5	d_{12}	165.5
$N_3(d_2)$	153	d_{13}	131
$N_4(d_3)$	181	d_{14}	160
$N_5(d_4)$	186	d_{15}	186
$N_6(d_5)$	170.5	d_{16}	187.5
$N_7(d_6)$	183	d_{17}	186
d_7	126	d_{18}	179.5
d_8	132	d_{19}	195.5
d_9	124.5	d_{20}	192.5
d_{10}	160.5	d_{21}	192.5
d_{11}	170.5		

The rest of the data are as follows: short-term storage cost per unit is CNY 0.42/car·h; penalty cost per unit of time for delayed arrival is CNY 10/car·h; carbon trading price is CNY 0.07/kg; short-term storage time at nodes in the low season is 48 h; short-term storage time at nodes in the peak season is 144 h; exemption period at nodes is 24 h; carbon dioxide emission allowance in the low season is 211,200 kg; carbon dioxide emission allowance in the high season is 88,800 kg. The data refer to the actual operation data of the company, the price of China's carbon trading market and the research of the paper [26].

5.2 Analysis of results

The model is based on the data of vehicle multimodal transport in off-peak sales seasons, and the algorithm is based on running under MATLAB R2022a (64-bit). The particle swarm size NP is set to 180, the number of iterations T_{max} is 180, the learning factor c_1 is 1.7, the learning factor c_2 is 1.7, the maximum inertia weight w_{max} is 3.5, and the minimum inertia weight w_{min} is 0.5. As shown in Fig. 6, using the IPSO algorithm, the data of off-season of sales reaches the convergence around iteration 55, and the data of peak season of sales reaches the convergence around iteration 74. Meanwhile, when using the IPSO algorithm, both sets of examples converge to the optimal scheme within 75 iterations. According to the setting of Eq. 20, taking the number of intermediate iterations of 75 as 37, the fixed weight w is obtained to be approximately 2.9. Therefore, referring to the above experimental background, with all other parameter Settings remaining unchanged, the inertia weight is set to a fixed value of 2.9 to verify the ability of the PSO algorithm. As shown in Fig. 6, using the PSO algorithm, the data of off-season of sales reaches the convergence around iteration 79, and the data of peak season of sales reaches the convergence around iteration 90.

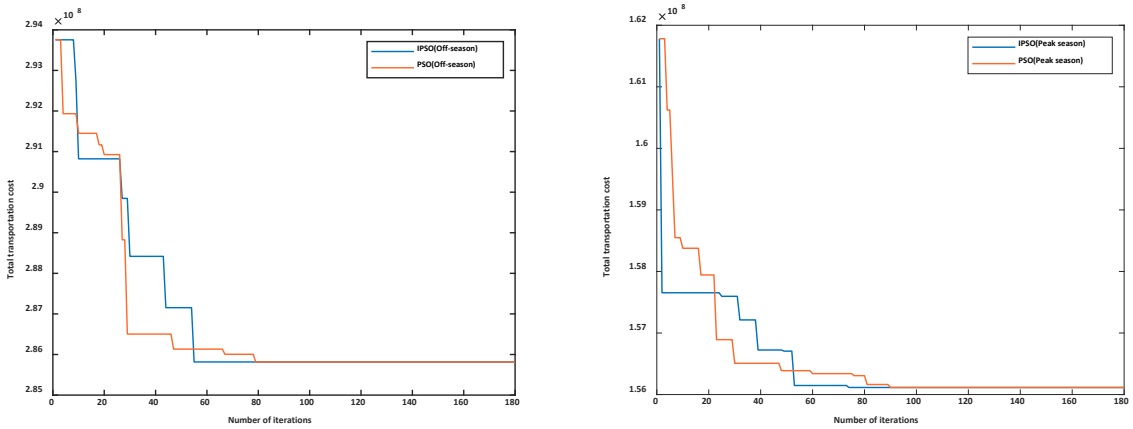

Fig. 6 Convergence of the objective function for sales off-peak seasons

Through comparison, both the IPSO algorithm and the PSO algorithm can converge to the optimal objective function within 100 iterations, proving that this algorithm can effectively solve the route optimization problem of whole vehicle multimodal transport. Meanwhile, compared with the PSO algorithm with a fixed inertia weight, the IPSO algorithm using a dynamic inertia

weight has reduced the number of convergences of the sales off-season examples by 30.38 % and those of the sales peak season examples by 17.78 %.

The optimal transport scheme for each dealer in the off-season is shown in Table 10, and the cost is accurate to a single digit. The total transport cost under the carbon trading policy is ¥2,858,013,466, and the unit transport cost of the vehicle is ¥1,893/car. The unit transportation cost of the reference enterprise during the off-season for vehicle sales is approximately ¥2,347/car. This plan reduces the total cost by 19.3 %. All the dealers' transport schemes use multimodal transport, with five dealers using road-rail-water multimodal transport and the rest using road-rail multimodal transport. More than half of the total number of dealers incurred time window penalty costs.

Table 10 Off-season vehicles transport scheme

Node	Transportation Path	C_1 (¥)	C_2 (¥)	C_3	C_4	C_5
$N_2(d_1)$	O-(2)-N_2-(1)-$N_2(d_1)$	17840	12623	1590	1499	5454
$N_3(d_2)$	O-(2)-N_3-(1)-$N_3(d_2)$	14171	63128	7954	5523	4258
$N_4(d_3)$	O-(2)-N_1-(3)-N_4-(1)-$N_4(d_3)$	23819	10036	4817	7168	2239
$N_5(d_4)$	O-(2)-N_1-(3)-N_5 -(1)-$N_5(d_4)$	19607	80514	3864	4984	1884
$N_6(d_5)$	O-(2)-N_6-(1)-N_6 (d_5)	32813	12672	1596	0	9822
$N_7(d_6)$	O-(2)-N_7-(1)-N_7 (d_6)	88507	27728	3493	0	2636
d_7	O-(2)-N_2-(1)-d_7	80328	42608	5368	8640	5043
d_8	O-(2)-N_2-(1)-d_8	75477	35648	4491	0	5536
d_9	O-(2)-N_2-(1)-d_9	53605	29304	3692	1029	3207
d_{10}	O-(2)-N_3-(1)-d_{10}	14377	56496	7118	8239	6510
d_{11}	O-(2)-N_3-(1)-d_{11}	36165	12264	1545	0	2202
d_{12}	O-(2)-N_3-(1)-d_{12}	28713	10584	1333	0	1502
d_{13}	O-(2)-N_2-(1)-d_{13}	20280	98768	1244	0	1433
d_{14}	O-(2)-N_3-(1)-d_{14}	14053	57432	7236	8056	5722
d_{15}	O-(2)-N_1-(3)-N_4-(1)-d_{15}	77598	28173	1352	1751	7996
d_{16}	O-(2)-N_1-(3)-N_4-(1)-d_{16}	44100	15435	7408	9154	4633
d_{17}	O-(2)-N_1-(3)-N_4-(1)-d_{17}	29370	10693	5132	6642	3022
d_{18}	O-(2)-N_6 -(1)-d_{18}	67891	23240	2928	0	3030
d_{19}	O-(2)-N_7 -(1)-d_{19}	12029	32512	4096	0	5721
d_{20}	O-(2)-N_7 -(1)-d_{20}	43455	12248	1543	0	1859
d_{21}	O-(2)-N_7 -(1)-d_{21}	18628	52240	6582	0	8079

The optimal transport scheme for each dealer during the peak sales season is shown in Table 11, with costs to the nearest digit. The total transport cost under the carbon trading policy is ¥156,108,521, and the unit transport cost of the vehicle is ¥2,548/car. The unit transportation cost of complete vehicles during the peak season for reference enterprises is approximately ¥2,990/car. This plan reduces the total cost by 14.8 %. 10 dealers exist that use full road transport, which is close to half of the total, and incur only transport and carbon emission costs. Of the dealers that choose multimodal transport, five use road-water transport and the rest use road-rail transport, all incurring time-window penalty costs.

During the peak sales season, the unit transport cost of the vehicle rose by 34.6 % compared to the off-season. The proportion of transport costs across various quarters surpasses 80 %, while there is a large variation in the transport scenarios and the proportion of remaining categories of costs. Refer to Fig. 7. Under schedule constraints, extended short-term storage durations at nodes during peak sales periods will markedly elevate both the time window penalty cost and the short-term storage cost, thereby diminishing the transport cost benefits associated with multimodal transport options. To minimize short-term storage links, the dealers who choose road-rail-water multimodal transport in the off-season switch to road-water multimodal transport in the peak season. Additionally, over half of the dealers utilizing road-rail multimodal transport switch to full road transport. After ignoring schedule restrictions, all dealers employ multimodal transport solutions throughout both off-season and peak seasons. In the off-season, road-rail-water multimodal transport is utilized, which shifts to road-water multimodal transport during the peak sales season. Additionally, orders placed by all dealers in the off-season do not incur time-window penalty costs, while such costs are elevated in the peak sales season.

Consequently, variations in peak and off sales seasons, along with schedule constraints, will influence transport options. Longer short-term storage times will force multimodal transport to shift to road transport to reduce the impact of short-term storage links. Simultaneously, schedule constraints exacerbate overall transit time, compelling multimodal transport to transition to road transport to mitigate the effects of waiting for the nearest schedule.

Table 11 Peak season vehicles transport scheme

Node	Transportation Path	C_1 (¥)	C_2 (¥)	C_3	C_4	C_5
$N_2(d)_1$	O-(1)-N_2-(1)-$N_2(d_1)$	11891642	0	0	0	210
$N_3(d)_2$	O-(1)-N_3-(1)-$N_3(d_2)$	9049380	0	0	0	160
$N_4(d)_3$	O-(1)-N_1-(3)-N_4-(1)-$N_4(d_3)$	13930768	3616	506	542	251
$N_5(d)_4$	O-(1)-N_1-(3)-N_5-(1)-$N_5(d_4)$	8236637	2099	293	291	148
$N_6(d)_5$	O-(2)-N_6-(1)-$N_6(d_5)$	13797862	5328	335	442	413
$N_7(d)_6$	O-(2)-N_7-(1)-$N_7(d_6)$	3720595	1165	734	903	110
d_7	O-(1)-N_2-(1)-d_7	4859526	0	0	0	844
d_8	O-(1)-N_2-(1)-d_8	4412788	0	0	0	762
d_9	O-(1)-N_2-(1)-d_9	3273424	0	0	0	570
d_{10}	O-(1)-N_3-(1)-d_{10}	8789320	0	0	0	154
d_{11}	O-(1)-N_3-(1)-d_{11}	2122411	0	0	0	369
d_{12}	O-(1)-N_3-(1)-d_{12}	1724579	0	0	0	301
d_{13}	O-(1)-N_2-(1)-d_{13}	11964217	0	0	0	206
d_{14}	O-(1)-N_3-(1)-d_{14}	8718881	0	0	0	153
d_{15}	O-(1)-N_1-(3)-N_4-(1)-d_{15}	4359753	1014	142	141	776
d_{16}	O-(1)-N_1-(3)-N_4-(1)-d_{16}	2456179	5562	778	755	436
d_{17}	O-(1)-N_1-(3)-N_4-(1)-d_{17}	1652939	3855	539	536	294
d_{18}	O-(2)-N_6-(1)-d_{18}	2855863	9776	615	725	127
d_{19}	O-(2)-N_7-(1)-d_{19}	5058640	1367	861	894	240
d_{20}	O-(2)-N_7-(1)-d_{20}	1827930	5152	324	350	782
d_{21}	O-(2)-N_7-(1)-d_{21}	784520	2200	138	150	340

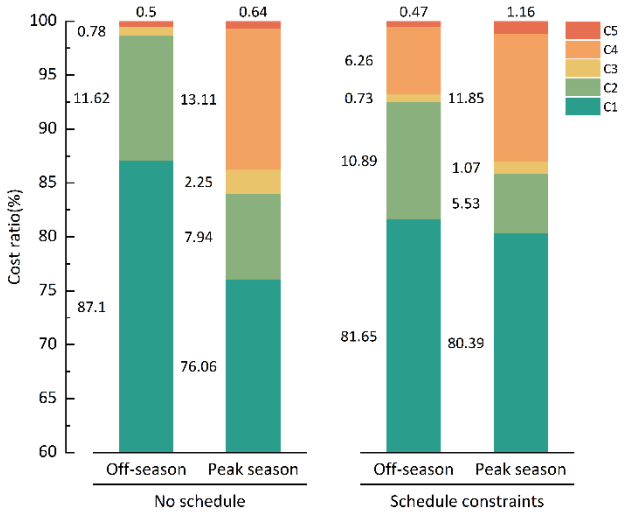

Fig. 7 Proportion of various costs in different scenarios

5.3 Sensitivity analysis

The generation of dealer demand orders is not fixed, and to explore the impact of different order shipping moments on the shipping scheme, orders are set to be shipped at 12 h intervals during the week. Fig. 8 illustrates the total cost and time cost associated with various shipping moments. There are two scenarios for different shipping moments: waiting for the nearest schedule and missing the nearest schedule, which will lead to a difference of the whole transport time, thus affecting the penalty cost of the time window as well as the total cost, and ultimately affecting the optimal route choice. Table 12 shows that under different shipping moments, the dealer's transportation path will also be affected.

Therefore, different shipping moments will affect the dealer transport scheme, and planning a reasonable shipping moment can effectively control the total cost, while proving that the fluctuation of the time window penalty cost will affect the optimal path selection.

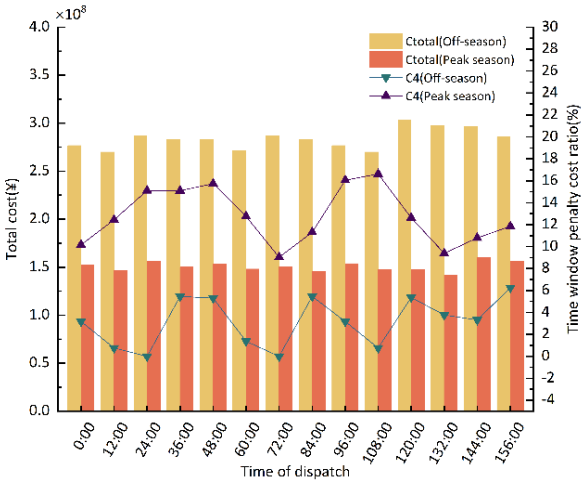

Fig. 8 Distributor total cost and proportion of time cost under different shipping moments

Table 12 Transportation schemes of some dealers under different shipping moments

Season	Time of dispatch	Transportation Path
Off-season	0:00; 12:00 …	O-(2)-N_1-(3)-N_4-(1)-N_4(d_3)
	24:00; 72:00 …	O-(1)-N_1-(3)-N_4-(1)-N_4(d_3)
Sales season	0:00; 12:00 …	O-(1)-N_1-(3)-N_4-(1)-d_{17}
	24:00; 36:00 …	O-(2)-N_6-(1)-d_{17}
Sales season	12:00; 24:00 …	O-(2)-N_3-(1)-N_3(d_2)
	0:00; 72:00 …	O-(1)-N_3-(1)-N_3(d_2)

In the actual operation of enterprises, sometimes the time requirements of dealer orders will be increased, and the time window limit will be stricter. To explore the impact of different time window ceilings on the transport program, selected the base data of 156:00 shipments in the off sales season, adhering to Upper limit of the time window under standard limitation requirements, executed by reducing progressively the time window by 10 percent incrementally. Fig. 9 illustrates the findings. As the degree of order expediting rises, total costs exhibit an upward trend; the proportion of selecting the road transport scheme demonstrates a stepwise increase; the proportion of time window penalty costs displays a fluctuating rise. As the level of order expediting rises, road-rail-water multimodal transport evolves into road-water multimodal transport or complete road transport, resulting in a progressive transformation of transport programs from near to far dealers. As shown in Table 13, new dealers' marks added from the initial stage are in red. In the first shift to road transport only, dealers such as d1, d7, and d8 are closer to the supplier, and as the distance of the transport route grows, dealers such as d2 and d5, which are farther away from the supplier, gradually shift to road transport only.

Therefore, different dealer time window ceilings will affect the dealer transport scheme choice, and as order expediting will force multimodal transport to shift to road transport to avoid excessive time window penalty costs, further proving that fluctuations in time window penalty costs will affect the optimal route choice. The distance between the dealer and the manufacturer will influence the selection of the transport scheme. With an increase in transport distance, multimodal transport offers a greater advantage in terms of transport cost.

In this paper, the carbon trading price is set at CNY 70/t according to the average price in China's carbon trading market. Currently, the average carbon pricing in different regions of the world is much higher than the Chinese carbon trading price [27]. To explore the impact of different carbon trading on the transport scheme within a reasonable range, the base data of 156:00 shipment in the peak selling season is selected, the carbon trading price was steadily raised by 0.1 yuan/kg from an initial value of 0 yuan/kg for research. As shown in Fig. 10. With the increase of carbon trading price, the total cost shows an incremental trend; the proportion of

choosing multimodal transport solutions shows a step-up trend; carbon emissions show a step-down trend, which is negatively related to the proportion of choosing multimodal transport solutions. With the increase of carbon trading price, the dealers who choose road transport only will gradually change to multimodal transport, and the programs of the transport distance from far to near dealers successively change. When the carbon trading price reaches CNY 1.30/kg, the carbon trading price can no longer play a regulatory role. As shown in Table 14, the new dealers added in the more initial stage are marked in red.

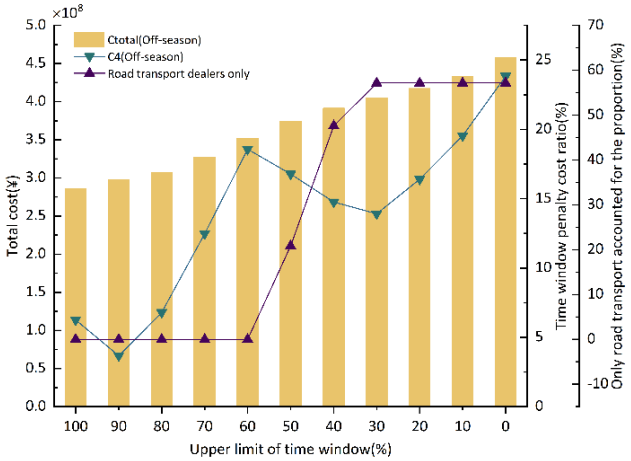

Fig. 9 Dealer related data in the upper limit of different time windows

Table 13 Road transport dealers only in the upper limit of different time windows

Upper limit of time window (%)	Proportion of road transport only (%)	Road transport dealers only
100–60	0	-
50	20.83	d_1, d_7, d_8, d_9, d_{13}
40	47.61	d_2, d_{10}, d_{11}, d_{12}, d_{14}
30–0	57.14	d_5, d_{18}

The results show that different carbon trading prices will affect the choice of transport options for dealers, and that an increase in carbon trading prices will effectively promote the transformation of road transport into multimodal transport, which will make the transport options greener and lower-carbon, but at the same time it will cause an increase in the total cost and increase the cost burden on the carriers. Consequently, it is further shown that transport distance influences the selection of transport options. Multimodal transport offers reduced carbon emissions, and its selection by dealers for extended transport distances can enhance this benefit, leading to decreased carbon costs and overall expenses

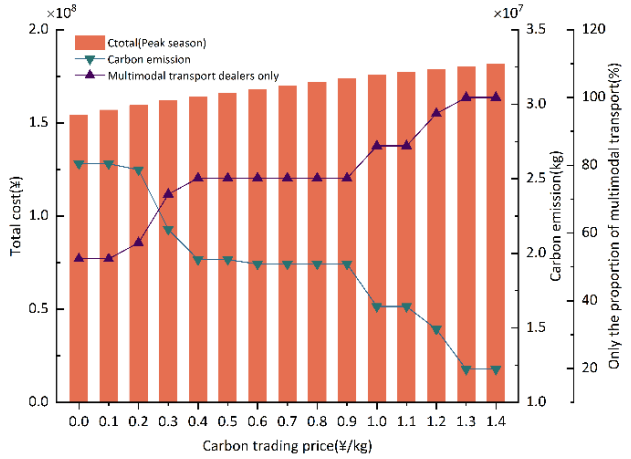

Fig. 10 Transport by distributors with different carbon trading costs

Table 14 Multimodal transport-only distributors with different carbon trading prices

Carbon trading cost (¥/kg)	Proportion of multimodal transport only (%)	Multimodal transport dealers only
0.0–0.1	52.38	d_3, d_4, d_5, d_6, d_{15}, d_{16}, d_{17}, d_{18}, d_{19}, d_{20}, d_{21}
0.2	57.14	d_{11}
0.3	71.43	d_{10}, d_{12}, d_{14}
0.4-0.9	76.19	d_2
1.0-1.1	85.71	d_8, d_{13}
1.2	95.24	d_7, d_9
1.3-1.4	100.00	d_1

6. Conclusion

This paper examines the optimization of multimodal transport paths for vehicles, considering schedule constraints within the framework of carbon trading policy. This study examines the impact of various factors, including sales off-peak season cache processing capacity, order timing demand, shift waiting, and carbon emissions, on transport schemes. We develop a multimodal transport path optimization model for vehicles, incorporating schedule constraints within the framework of carbon trading policy. The model seeks to minimize total transportation costs while adhering to constraints related to timetable periods, time windows, route flows, and node capacities. A particle swarm algorithm incorporating a dynamic inertia weight and a linear weight reduction strategy is proposed. The effectiveness of the model and algorithm is demonstrated through a real-world case study of vehicle multimodal transport in China. The results indicate that transport timeliness significantly influences optimal path selection. Extended short-term storage duration, increased shift waiting time for shipping, expedited orders, and other factors compel multimodal transport to transition to road transport to mitigate excessive time window penalty costs. Increasing the carbon trading price will effectively encourage a transition from road transport to multimodal transport, thereby enhancing the low-carbon nature of the transport scheme. However, too high a carbon trading price will not be able to play a regulatory role, and at the same time will cause the total cost to increase, necessitating a careful and reasonable price setting. Additionally, the transport distance influences the selection of transport schemes. When the order time requirement is shortened, dealers tend to prefer road transport for shorter distances. Conversely, when carbon emission costs are elevated, dealers are more likely to opt for multimodal transport over longer distances.

In the future, our further research will focus on the capacity scheduling of time-varying multimodal transport networks and the hybrid transport mode involving multiple automakers to improve the potential of the model in solving complex scenarios in the real world and try to utilize the analysis from a multi-objective optimization perspective.

References

[1] Shao, S., Tan, Z., Liu, Z., Shang, W. (2022). Balancing the GHG emissions and operational costs for a mixed fleet of electric buses and diesel buses, *Applied Energy*, Vol. 328, Article No. 120188, doi: 10.1016/j.apenergy.2022.120188.

[2] Zhang, Y., Zhang, A., Wang, K., Zheng, S., Yang, H., Hong, J. (2023). Impact of CR express and intermodal freight transport competition on China-Europe route: Emission and welfare implications, *Transportation Research Part A: Policy and Practice*, Vol. 171, Article No. 103642, doi: 10.1016/j.tra.2023.103642.

[3] Chen, W., Zhang, L., Shi, L., Shao, Y., Zhou, K. (2022). Carbon emissions trading system and investment efficiency: Evidence from China, *Journal of Cleaner Production*, Vol. 358, Article No. 131782, doi: 10.1016/j.jclepro.2022.131782.

[4] Zhang, X., Guo, A., Ai, Y., Tian, B., Chen, L. (2022). Real-time scheduling of autonomous mining trucks via flow allocation-accelerated tabu search, *IEEE Transactions on Intelligent Vehicles*, Vol. 7, No. 3, 466-479, doi: 10.1109/TIV.2022.3166564.

[5] Sarnvanichpitak, T., Mangmeechai, A. (2024). Regional differences in car sharing adoption: Integrating TAM and TPB in Bangkok and Eastern Economic Corridor, Thailand, *Journal of Logistics, Informatics and Service Science*, Vol. 11, No. 12, 71-89, doi: 10.33168/JLISS.2024.1204.

[6] Khadka, P.B., Karki, D., Dahal, R.K., Khanal, D. (2024). Mapping the landscape of green finance and banking performance research: A bibliometric analysis, *Journal of Service, Innovation and Sustainable Development*, Vol. 5,

No. 1, 176-193, doi: 10.33168/SISD.2024.0110.
[7] Elbert, R., Mueller, J.P., Rentschler, J. (2020). Tactical network planning and design in multimodal transportation – A systematic literature review, *Research in Transportation Business and Management*, Vol. 35, Article No. 100462, doi: 10.1016/j.rtbm.2020.100462.
[8] Peng, Y., Gao, S.H., Yu, D., Xiao, Y.P., Luo, Y.J. (2023). Multi-objective optimization for multimodal transportation routing problem with stochastic transportation time based on data-driven approaches, *Rairo-Operations Research*, Vol. 57, No. 4, 1745-1765, doi: 10.1051/ro/2023090.
[9] Zhang, Z., Li, D., Meng, J., Jiang,, M. (2022). Multi-objective multimodal transport path optimization model and algorithm considering carbon emissions, In: *Proccedings of 2022 2nd International Conference on Algorithms, High Performance Computing and Artificial Intelligence (AHPCAI),* Guangzhou, China, 80-84, doi: 10.1109/ AHPCAI57455.2022.10087489.
[10] Kurnia, A., Oktavia, T. (2024). A multi-criteria decision approach for optimized route planning in retail distribution, *Journal of Logistics, Informatics and Service Science*, Vol. 11, No. 9, 37-53, doi: 10.33168/JLISS.2024.0903.
[11] Pătraşcu, A., Toader, F.A., Bălăcescu, A. (2024), An improved multi-objective hybrid algorithm for solving job shop scheduling problem, *Economic Computation and Economic Cybernetics Studies and Research,* Vol. 58, No. 3, 177-192, doi: 10.24818/18423264/58.3.24.11.
[12] Liu, S., Zhang, C. (2021). Optimization of urban cold chain transport routes under time-varying network conditions, *Journal of Advanced Transportation*, Vol. 2021, No. 1, Article No. 8817991, doi: 10.1155/2021/8817991.
[13] Zhao, W. (2021). Optimal fixed route for multimodal transportation of vehicle logistics in context of soft time windows, *Scientific Programming*, Vol. 2021, No. 1, Article No. 2657918, doi: 10.1155/2021/2657918.
[14] Liu, T. (2024). Time-varying influence of policy risk on carbon emissions analysis, *Journal of Service, Innovation and Sustainable Development*, Vol. 5, No.2, 95-115, doi: 10.33168/SISD.2024.0206.
[15] Ji, X., Xu, W., Aslam, R., Yin, Y. (2024), The influence of government on automobile enterprise`s production methods: An evolutionary game based study, *Economic Computation and Economic Cybernetics Studies and Research*, Vol. 58, No. 4, 223-240, doi: 10.24818/18423264/58.4.24.14.
[16] Somsai, T., Pongcharoen, P., Hicks, C. (2024). Optimizing sustainable multimodal distribution networks in the context of carbon pricing, with a case study in the Thai sugar industry, *Energy*, Vol. 298, Article No. 131273, doi: 10.1016/j.energy.2024.131273.
[17] Wang, D.L., Ding, A., Chen, G.L., Zhang, L. (2023). A combined genetic algorithm and A* search algorithm for the electric vehicle routing problem with time windows, *Advances in Production Engineering & Management*, Vol. 18, No. 4, 403-416, doi: 10.14743/apem2023.4.481.
[18] Liu, M.L., Zhang, C., Wu, Q.L., Meng, B.R. (2021). Vehicle routing problem with soft time windows of cargo transport O2O platforms, *International Journal of Simulation Modelling*, Vol. 20, No. 2, 351-362, doi: 10.2507/IJSIMM20-2-564.
[19] Shoukat, R., Zhang, X. (2023). Sustainable logistics network optimization from dry ports to seaport: A case study from Pakistan, *Transportation Research Record: Journal of the Transportation Research Board*, Vol. 2677, No. 3, 302-318, doi: 10.1177/03611981221115121.
[20] Wang, J., Wu, D., Wang, X. (2018). Urban multimodal transportation system simulation modeling considering carbon emissions, In: *Proceedings of 2018 30th Chinese Control and Decision Conference (CCDC),* Shenyang, China, 3040-3045, doi: 10.1109/CCDC.2018.8407646.
[21] Wang, Z.J., Suo, J. (2022). Optimization of flexible production logistics under low carbon constraint, *International Journal of Simulation Modelling*, Vol. 21, No. 1, 184-195, doi: 10.2507/IJSIMM21-1-CO5.
[22] Yin, C., Zhang, Z.-A., Fu, X., Ge, Y.-E. (2024). A low-carbon transportation network: Collaborative effects of a rail freight subsidy and carbon trading mechanism, *Transportation Research Part A: Policy and Practice*, Vol. 184, Article No. 104066, doi: 10.1016/j.tra.2024.104066.
[23] Li, K., Li, D., Ma, H.Q. (2023). An improved discrete particle swarm optimization approach for a multi-objective optimization model of an urban logistics distribution network considering traffic congestion, *Advances in Production Engineering & Management*, Vol. 18, No. 2, 211-224, doi: 10.14743/apem2023.2.468.
[24] Arasomwan, M.A., Adewumi, A.O. (2013). On the performance of linear decreasing inertia weight particle swarm optimization for global optimization, *The Scientific World Journal*, Vol. 2013, No. 1, Article No. 860289, doi: 10.1155/2013/860289.
[25] Zheng, D. (2020). *Research on optimization of passenger car intermodal transport network considering carbon emissions,* MS thesis*,* Dalian University of Technology, Dalian, China, doi: 10.26991/d.cnki.gdllu.2020.004659.
[26] He, B. (2020). *Design of a multimodal transport scheme for full truckloads of Fengshen logistics considering carbon emissions,* MS thesis, Changsha University of Science and Technology, Changsha, China, doi: 10.26985/d.cnki.gcsjc.2020.000290.
[27] Xu, L., Yang, J. (2024). Carbon pricing policies and renewable energy development: Analysis based on cross-country panel data, *Journal of Environmental Management,* Vol. 366, Article No. 121784, doi: 10.1016/j.jenvman.2024.121784.